Meteorologische Zeitschrift, Vol. 24, No. 6, 547–555 (published online April 13, 2015)

ISARS 17

Remote sensing winds in complex terrain – a review

Stuart Bradley[1]*, Alexander Strehz[1] and Stefan Emeis[2]

[1]University of Auckland, Physics Department, Auckland, New Zealand
[2]Karlsruhe Institute of Technology, Institute of Meteorology and Climate Research – Atmospheric Environmental Research, Garmisch-Partenkirchen, Germany

(Manuscript received August 11, 2014; in revised form December 16, 2014; accepted December 16, 2014)

Abstract

Ground-based remote sensing is now essential for wind energy purposes. Currently available remote sensing instruments construct a wind vector from wind components measured at several spatially separated volumes, leading to errors on complex terrain where the flow is inhomogeneous. Wind estimation errors are found to be fully described by only two parameters: the flow curvature and flow inclination above the instrument. However, neither parameter is measured directly, nor are they simple products of flow models, so the challenge is to adequately estimate them. Linearized flow models are attractive in being fast and requiring few inputs, but make several limiting assumptions that can lead to their failure to adequately predict corrections for remote sensing. It is found that sophisticated CFD models can also over-correct. The status of such corrections is reviewed here, from a number of diverse measurement campaigns, and it is found that generally remote sensed winds can be corrected to within 1.5 % of nearby mast winds. Alternative methods, using multiple receivers sensing several wind components within one volume, are also reviewed. Such systems show promise but are under development and further improvements are likely.

Keywords: remote sensing, complex terrain, wind profiles, inhomogeneous wind fields, wind error correction

1 Introduction

Wind turbines are increasingly erected in orographically complex terrain, and new turbine designs are becoming taller. The current state of the art for modelling air flow near the ground in complex terrain is not sufficiently accurate as a stand-alone method. An example is the challenge presented to even very sophisticated models by the small and low Bolund peninsula (Bechmann et al., 2011; Berg et al., 2011; Diebold et al., 2013; Prospathopoulos et al., 2012; Vuorinen et al., 2015). It is possible that such models will never achieve the required accuracy due to the complexity of inputs required. Therefore it is necessary to perform measurements in order to accurately characterise the wind field.

Remote sensing of wind profiles is needed for two reasons: (1) the spatial representativeness of a single profile measurement in horizontally inhomogeneous flow is rather low, and (2) tall masts reaching up to modern hub heights of more than 100 m are very expensive, and even more expensive for measuring winds over the whole swept area of a turbine. This combination means that mobility of the measurement instrumentation is important, and direct measurements are no longer viable (Emeis et al., 2007).

Remote sensing by acoustic or optical means is a very favourable option to measure such wind profiles. The most common instruments (mono-static sodar or wind lidar) either use the Doppler beam swinging (DBS) technique or do conical scanning within the air volume of interest in order to obtain all three components of the three-dimensional wind vector. A common prerequisite to both techniques is the assumption of horizontal homogeneity. This homogeneity does not exist in orographically complex terrain. The result is that uncorrected estimates of wind using common remote sensing instruments can be in error by typically up to 6 % of the wind speed (Behrens et al., 2012), which is also unacceptable for wind energy applications.

The solution is either to correct the remote sensing data for the inhomogeneities or to design other measurement techniques which do not rely on this homogeneity. This review will address both options.

Correction is possible if it is assumed that the remote sensing measurements can be input into a wind flow model so that the wind above the measurement site is calculated with more accuracy than provided by the measurements alone. High-resolution numerical flow models (Ayotte, 2008; Bechmann and Sørensen, 2010; Bezault et al., 2012; Butler and Quail, 2012; Harris et al., 2010; Jackson et al., 2011; Jafari et al., 2012; Friman, 2011; Pitter et al., 2012; Prospathopoulos et al., 2012; Rasouli and Hangan, 2013; Xu et al., 2013) have detailed orography and land use data as input for the lower boundary condition of the flow, but are very costly and time-consuming. While CFD and LES models have been intensively researched as methods for correcting remotely sensed winds, the required corrections are generally second-order (< 6 %), and influenced primarily by terrain at the measurement

*Corresponding author: Stuart Bradley, University of Auckland, Physics Department, Private Bag 92019, Auckland, New Zealand, e-mail: s.bradley@auckland.ac.nz

site (Jeannotte et al., 2014; Wakes et al., 2010). Thus correction methods might better be based on: existing experiments which investigated flow over orography (Bradley et al., 2012b; Lang and McKeogh, 2011); simple flow models for the given measurement site (e.g. Bradley, 2007, 2012); assumptions on linearly varying wind components (Bingöl et al., 2009a); or on a dimensional analysis. This is not true, of course, for extreme situations where there is flow separation (Palma et al., 2008), and in general there are decisions required as to the degree of complexity the site might involve (Wakes et al., 2010).

Other remote sensing techniques could involve enhanced analysis techniques, such as making use of information from more than three measurement volumes to correct for wind gradients (Behrens et al., 2010), bistatic sodars and lidars (Bradley et al., 2012a; Strehz and Bradley, 2014), or 'virtual towers' constructed from multiple Doppler lidars (Foussekis et al., 2009). A very different approach is to use a lidar system which obtains wind components from the lag time of the best correlation between the returns from two laser beam having a separation angle of, say, 10 ° (Afek et al., 2013). The small angular separation of lidar beams, and measuring the time taken for recognisable air patches to move from one beam to another, means that some sources of error in inhomogeneous wind fields will be absent. However, it is not clear from the supplier's data how vertical wind components are measured by this non-Doppler system and, if vertical components are not measured then, in a complex terrain environment there may be substantial errors arise.

This paper starts with the description of the general problem of remote wind profile measurements in complex terrain in Section 2. Estimations of the error in wind measurements from potential flow considerations and a dimensional analysis are presented in Section 3, while Section 4 discusses corrections using CFD flow models. Sensing wind vector components within a single volume by using multiple receivers is discussed in Section 5. Existing experimental results are summarized in Section 6 followed by Conclusions.

2 The problem

The problem for volume-averaging remote wind vector measurements in complex terrain is described in Fig. 1 which also serves for the definition of the used notation. A similar approach is given by Rovers (2012), who also treats measurements in a valley. The graphs each show two slanted beams, each tilted at an angle α to the vertical. These beams can be seen either as two separate beams emitted under the DBS technique or as two extreme positions during conical scanning.

The remote sensing instrument measures the radial wind component V_{r-} with the left-hand beam and the radial component V_{r+} with the right-hand beam. In its simplest form, processing to obtain an estimate of the horizontal wind component, u, is via

$$\hat{u} = \frac{V_{r+} - V_{r-}}{2 \sin \alpha}. \tag{2.1}$$

For flat terrain and a horizontal streamline, $V_{r+} = -V_{r-} = u \sin \alpha$ so $\hat{u} = u$. For straight-line flow tilted at an inflow angle β, $V_{r+} = V \sin(\alpha + \beta)$ and $V_{r-} = -V \sin(\alpha - \beta)$, so again $\hat{u} = u$. However, for curved flow symmetric above the instrument (e.g. over the ridge or a hill), the vertical wind component is upward on the upstream side and downward on the downstream side. Here $V_{r+} = V \sin(\alpha + |\beta|)$ and $V_{r-} = -V \sin(\alpha - |\beta|)$, where β is the angle of the flow to the horizontal (the inflow angle). This gives

$$\hat{u} = u \left(\cos |\beta| - \frac{\tan |\beta|}{\tan \alpha} \right).$$

Let R be the radius of curvature of the streamline i.e. the curved streamline is locally an arc of a circle of radius R. The slope of this arc at the measurement points is $\pm \tan \beta$, as shown in Fig. 2. This means that $D = R \sin \beta = z \tan \alpha$ and, since $\beta \ll 1$,

$$\hat{u} = u \left(1 - \frac{z}{R} \right). \tag{2.2a}$$

More generally, for curved streamlines which are also sloping at a mean angle β_0 above the instrument,

$$\hat{u} = u \left(1 - \frac{z}{R \cos \beta_0} \right). \tag{2.2b}$$

Equation (2.2) demonstrates three important features. The first is that, in the *linear flow regime*, $\hat{u} = u(1 + \varepsilon)$ where ε describes the geometry through a number of dimensionless parameters (here, only z/R). This means that the fractional error remains the same, regardless of the strength of the wind. The second feature is that the correction is independent of the instrument cone angle α. This is related to α being small enough that $\sin \alpha \approx \alpha$ (for $\alpha = 20\,°$, $\alpha / \sin \alpha = 1.02$). The third feature of (2.2) is that errors arise only through the *curvature* of the streamlines. An instrument placed on the side of a hill, rather than on the ridge, will still have errors entirely dependent on the curvature, and independent of the mean upslope flow angle.

Corrections for measurements at the hill peak require an estimate of the radius of curvature R of the streamline at height z. Curvature is a measure of terrain complexity, as is the maximum hill slope. Models for correcting remote sensing wind estimates based on field data have maximum hill slopes varying between 0.1 (Bradley, 2012; Jeannotte et al., 2014; Wakes et al., 2010) to 0.3–0.4 (Behrens et al., 2010; Harris et al., 2010) and typical measurement heights are $z = 80\,\mathrm{m}$ and hill height $H = 200\,\mathrm{m}$. For a Gaussian-shaped hill (Feng and Shen, 2014), the relative wind estimation error is $\varepsilon = -2.7(\text{maximum slope})^2(z/H)$. If it is assumed that

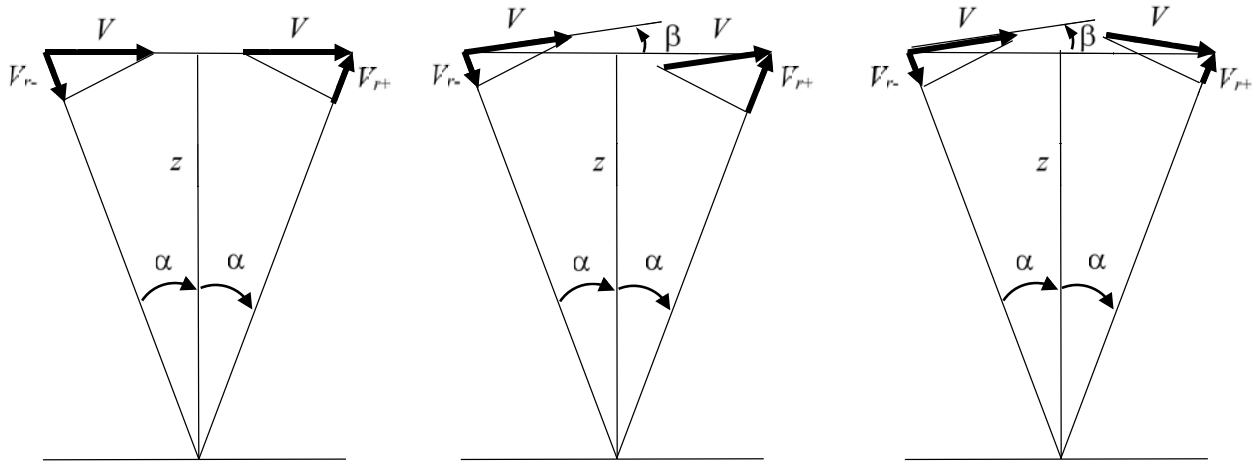

Figure 1: Left: Mono-static remote sensing of the horizontal wind vector in flat terrain with the wind horizontal. Centre: Mono-static remote sensing on the side of a hill, with straight stream-lines tilted at an inflow angle β to the horizontal. Right: Mono-static remote sensing on a hill top, with curved streamlines tilted at an inflow angle of $+\beta$ at the upwind sensing volume and at $-\beta$ at the downwind sensing volume.

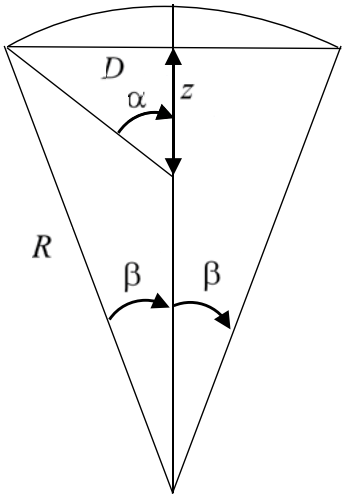

Figure 2: The geometry for a streamline which is a circular arc of radius R.

the streamlines follow parallel to the hill surface, the relative error predicted on the basis of the above analysis is in the range 1 %–14 %.

Remotely sensed winds can be corrected for hill curvature if R can be estimated. If there is an uncertainty σ_R in estimating R from a model, the relative uncertainty in the corrected estimation of u is $\sigma_u/u = (z/R)(\sigma_R/R)$ i.e. the wind estimation error is reduced by a factor σ_R/R. The relative uncertainty in R should be able to be estimated to within 10 %. This suggests that corrections should be possible to better than 1 % in most instances.

There are two gross simplifying assumptions in the above: that the wind speed is unchanged along a streamline (within the radius of the sampling cone); and that the streamlines are parallel to the hill surface. We now examine the validity of these assumptions in more detail.

3 Estimation of corrections from linear flow models

Flow inhomogeneities induced by orography and the impact of these inhomogeneities on remote sensing data can be described in the space domain (Fig. 3), if a few simplifying assumptions are made. First of all, it is assumed that the orography contours are so gentle that no flow separation takes place and attached flow occurs. In this case the curvature of the streamlines is similar to the curvature of the hill contour along a cross-section through the orography parallel to the flow direction. Furthermore, it is assumed the geometry of the flow does not depend on wind speed, as described above. The primary length scales are R and z.

Turbulent flow and atmospheric stability will affect the validity of these simplifying assumptions. Turbulence intensity of the flow either comes from surface roughness or from thermal instability. This introduces some more length scales: the mixing length, l, the surface roughness length, z_0, and the Monin-Obukhov length, L_*. These length scales allow for the formation of several non-dimensional numbers. A few of them just give known parameters. For instance, the ratio D/z is just the tangent of the opening angle, α, of the remote sensing device. The radius of curvature of the orography, R, is closely linked to two other commonly known orographic length scales, the hill height, H, and the half width of a hill, L (often measured at half hill height). If the hill contour is approximated by the arc of a circle segment, then H is the height of the arc over the chord and L is half the length of the chord. The cone angle, γ, is also related to these dimensions through $H = R(1-\cos\gamma)$ and $H/L = (1-\cos\gamma)/\sin\gamma$. Some examples of these relationships are listed in Table 1. Usually, flow separation starts somewhere between slopes of 0.2 and 0.3. Therefore, larger values for the slope than those given in Table 1 are not meaningful, because non-

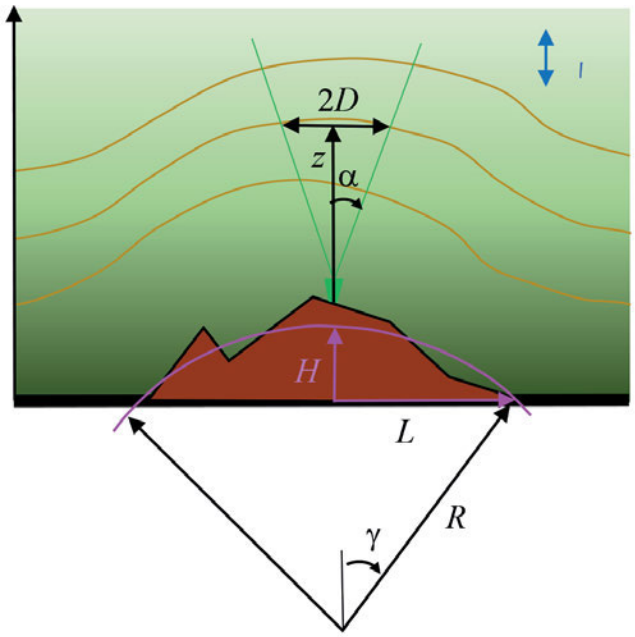

Figure 3: Some length scales relevant for remote sensing in complex terrain. The orography (brown) is characterized by the hill height, H, the half width of the hill, L, and the radius of curvature, R. The ratio L/R is related to the sector angle γ. The measurement (green) is characterized by the half opening angle of the remote sensing device, α, and the measurement height, z. α and z together define the width, $2D$, of the measurement volume at height z. The turbulent state of the atmosphere (orange) is characterized by the mixing length, l, which in turn is a function of the Monin-Obukhov length, L_*.

Table 1: Relation between the tangent, H/L, of the terrain slope, the angles γ and β, the radius of curvature of the terrain, R, and the wind speed error ε in % for $L = 1000$ m, $D = 40$ m, and $z = 150$ m ($\alpha = 15°$).

$H/L =$ $(1-\cos\gamma)/\sin\gamma$	γ	R[m] = $H/(1-\cos\gamma)$	$\beta =$ $\sin^{-1}(D/R)$	$\varepsilon = z/R$
0.1	11 °	5050	0.5 °	−3.0 %
0.2	23 °	2600	0.9 °	−5.8 %
0.3	33 °	1820	1.3 °	−8.2 %

separating flow is assumed in this estimation, and installation of a turbine in a region of separating flow is not a good design decision. The case of a flow across a valley can be estimated by taking negative values for H. This then leads to negative values for the flow inclination β and positive values of the wind speed error.

Bradley (2012) and Bradley et al. (2012b) describe a flow model based on the streamlines generated by the classic inviscid irrotational (potential) flow over a cylinder. Streamlines further from the cylinder are less perturbed from a straight line and are close to a Gaussian shape. Any one of these streamlines can be chosen as being a hill surface, since there is no flow through a streamline. The remaining streamlines above the hill surface streamline then describe the flow in a relatively simple analytic way.

For example, chosing $H = 200$ m, $H/L = 0.3$, and a measurement height of $z = 80$ m above the ridge, gives the results in Fig. 4. The radius of curvature of the ridge is 1790 m and the radius of curvature of the streamline through the point 80 m above the ridge is 2620 m. The speed-up factor at 80 m above the ridge is 1.22. The measurement error ε is −4.5 % based on $R = 1790$ m and −3.1 % based on $R = 2620$ m, and also −3.1 % using actual values of V and β at the measurement locations.

It is clear that, even in this simple linear flow model, the streamline curvature is not the same as the underlying hill, and the wind speed is not constant along a streamline. However, for the example given above and plotted in Fig. 4, the wind speed at the two measurement points is 0.9997 of the speed directly above the ridge, so the assumption of the wind speed being constant along a streamline within the distance $2D$ is a good one. The advantage of an analytic model, though, is its ability to provide insight into the relevant scaling relationships. For example, the analytic potential flow model described above gives an explicit relationship for the speed-up above the ridge, u/U, and dimensionless parameters H/L and z/H, as follows

$$\frac{u(0)}{U} - 1 = 2\frac{1+k}{\left(1+k+2\frac{z}{H}\right)^2} \tag{3.1}$$

where $k^2 = 4(H/L)^{-2} - 2$, $u(0)$ is the wind speed directly above the ridge, and U is the undisturbed wind speed distant from the hill.

Although more sophisticated linear flow models inherently assume a neutral atmosphere and ignore turbulence, they have been very successful in providing corrections for remote sensing. These models derive from the classic work of Jackson and Hunt (1975) which allowed for a general topography shape and multiple atmospheric layers. Ayotte (2008) gives a review of both linear and non-linear models, with a discussion of their advantages and disadvantages. A very widely used modern model is the Wind Atlas Analysis and Application Program, or WAsP (Bingöl et al., 2009b,a; Harris et al., 2010; Jeannotte et al., 2014; Friman 2011; Mann et al., 2002; Mortensen et al., 2006; Palma et al., 2008; Wakes et al., 2010). The recommended maximum slope is 0.3 for use of this model although Mortensen et al., (2006) extends this in some instances to 0.40–0.45. Harris et al., (2010) describes a comparison between lidar measurements and a mast, together with corrections from WAsP and from a CFD model. Lidar errors were $\varepsilon = 0$ % to −4 %. The differences between lidar ε and WAsP correction vary with wind direction, but the average correction required for the lidar is around −3 % and predicted by WAsP around −4 %. The mean absolute difference in ε and WAsP correction was 2 %, but this may have been strongly influenced by some wind directions. It would seem linearized models are capable of correcting remote sensing winds to within 1 %–2 %, which may be an acceptable level for the industry.

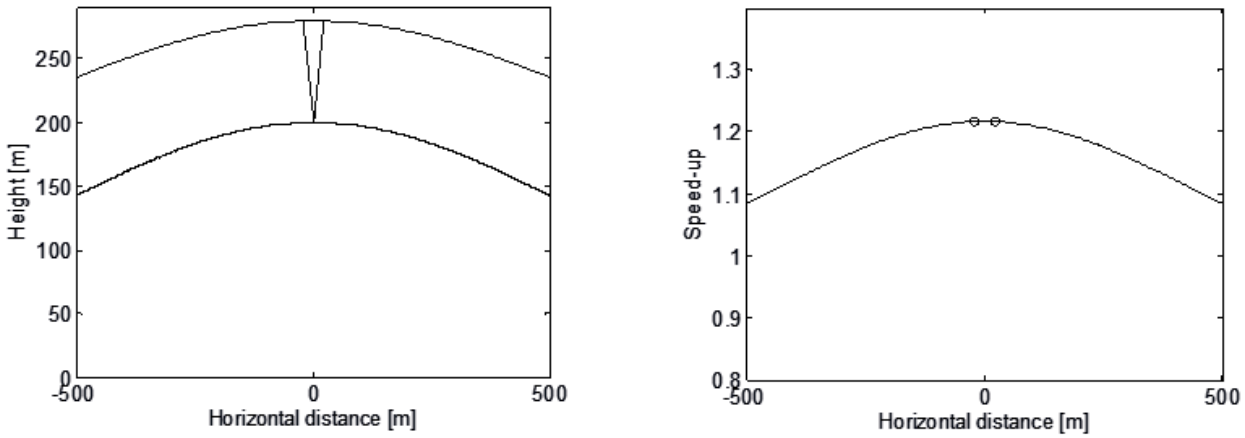

Figure 4: Potential flow solution for a hill of height $H = 200\,\text{m}$, and $H/L = 0.3$. Left plot: the hill surface (lower curved line) and streamline through a point 80 m above the ridge (upper curved line). Sensing directions shown for $\alpha = 15\,°$. Right plot: the speed-up factor along the streamline shown in the left plot. The sensed wind speeds are shown as circles for $\alpha = 15\,°$.

4 Corrections based on CFD and LES models

There are many CFD and LES models, but here we will concentrate on those which have been used to correct remote sensing data, rather than including also those which aim to provide stand-alone wind predictions. However, in some cases non-linear models have been used to predict the speed-up over idealised Gaussian hills, thus providing a point of comparison with the simple approximations described in Sections (2) and (3) above.

Ayotte (2008) has measured flow in a wind tunnel over a model Gaussian hill. The speed-up factor was then modelled using a linear model and a non-linear model. The non-linear model agreed with measurement much more closely. The speed-up with a hill of maximum slope equal to 0.3 was, from the linear model 0.72 and from measurements and the non-linear model 0.62. However, a flow model can obtain an estimate $\hat{\varepsilon}$ of the remote sensing fractional error, so the corrected remotely sensed wind is $u(0,z) = u_{\text{remote}}(0,z)/(1-\hat{\varepsilon})$. This means that the *absolute magnitude* of the wind speed is not important for correcting remotely sensed winds, but rather how much the streamline curvature affects the projection of the wind vector onto the radial beam direction.

Bezault et al. (2012) have modelled flow over complex terrain in New Zealand and Spain. For the New Zealand case, a fit to the E-W topography transect gave $R_{\text{EW transect}} \approx 2100\,\text{m}$. The measurements were on a ridge running from 220 ° to 40 ° and the flow was from 210 °. Allowing for these directions the effective $R_{\text{hill}} = 1350\,\text{m}$, $H = 150\,\text{m}$, and $L = 500\,\text{m}$. The simple potential flow model of Section 3 above gives the radius of curvature of the streamline through the $z = 80\,\text{m}$ measurement height as 2290 m. This gives a speedup of 20 %, compared with the CFD speedup of 15 %, and a correction factor of $\varepsilon = -0.034$ compared with the CFD correction factor of −5 %. The CFD corrections gave excellent agreement between lidar and mast. If the linear model had been used here, the corrected lidar winds would be 1.6 % too low.

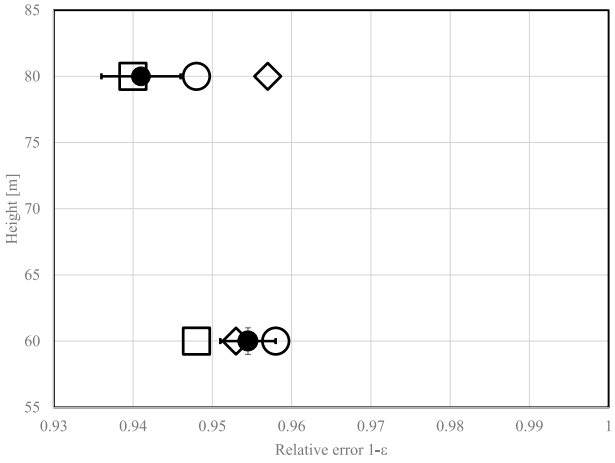

Figure 5: Comparison between measurements (solid circles), potential flow model (open circles), OpenFOAM CFD model (squares), and WindSim CFD model (diamonds) at a very complex site described by Behrens et al. (2012)

Behrens et al. (2012) conducted sodar and mast measurements in very complex terrain and compared results with predictions from the potential flow model of Section 3 above, with WindSim, a CFD solver using Reynolds-averaged Navier Stokes (RANS) turbulence closure, and with OpenFOAM (see http://www.openfoam.org/), an open-source CFD toolbox. Their results are reproduced in Fig. 5. The measured underestimation is typical of that discussed above, with underestimation larger at larger heights. The various models predict this underestimation to within about 0.8 % at a height of 60 m and to within about 1.5 % at 80 m. None of the models predict the underestimation to within the

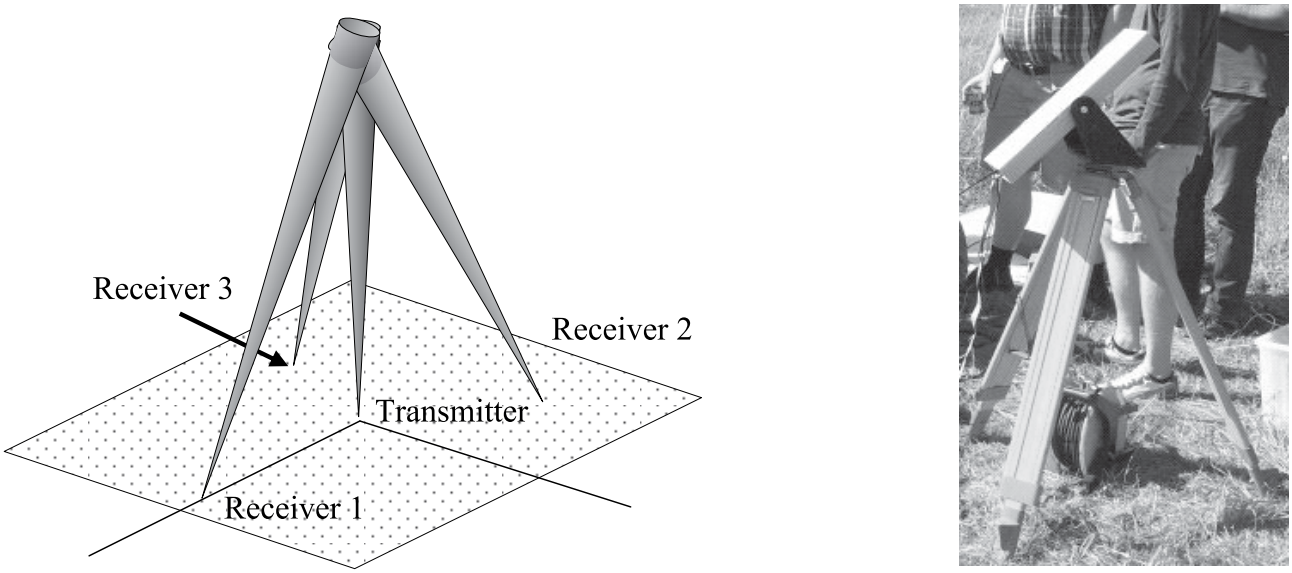

Figure 6: The basic geometry (left drawing) and one of the receivers (right photo) for the Auckland bistatic sodar (Strehz and Bradley 2014).

experimental errors at both heights. The RMS differences between model predictions and measurements are 0.6 %, 1.1 %, and 0.5 % for the potential flow model, WindSim, and OpenFOAM, respectively. There is no evidence that the CFD models perform better than the linear model, for correcting the sodar winds, in this example.

5 Vector wind measurements obtained from within a confined volume

The distributed sampling volume problem described above arises because all current comercial lidars and sodars are monostatic. 'Monostatic' means having the transmitter and receiver co-located, in contrast to 'bistatic' which means having physically separated transmitter and receiver (Bradley, 2007). Configurations such as WindScanner (Mikkelsen and Bradley, 2011), which involve multiple lidars, are also monostatic because each lidar involved is operating as a monostatic instrument. The monostatic configuration has the advantage of being compact and, in the case of sodars, also using a common transducer for both transmission and reception. It would be challenging to develop a bistatic lidar configuration because light scattering is primarily forward (which is inaccessible) or backward (the monostatic case), although there has been some development work on a bistatic lidar (Friman, 2011; Eggert, 2013). This limitation is not present for sound, since the scattering process is very different and in fact stronger scattering occurs at oblique angles. Recent developments in bistatic sodars are described by Bradley et al. (2012a) and Strehz and Bradley (2014).

These multiple receiver configurations obtain the three wind vector components from the same volume, as depicted in Fig. 6. In the case of the bistatic sodar the Doppler shift is generally greater than the monostatic case because the projection of the wind vector onto the receiver beam axis direction is larger. An example from a prototype bistatic sodar in very complex terrain is shown in Fig. 7. The number of samples here is not large, and the corresponding coefficient of determination R^2 is low compared with typical values obtained on flat terrain. However, it can be seen that in this terrain the monostatic sodar underestimates the wind speed by 6 % whereas the bistatic sodar is within 0.5 % of the mast wind speeds. The small offset (−0.2 m/s) may be due to both the monostatic and bistatic sodars not being situated directly beneath the mast. There is a penalty with these multiple-receiver systems: the receivers are spread laterally by around 40 m. This means that cabling and finding suitable sites, particularly in forested terrain, can be challenging, because there are at least four installations required.

Continuous bistatic sodar measurements have also been made (Mikkelsen et al., 2007), This method needs refinement to be useful, but has the potential for real-time turbulence and gust measurements.

6 Experimental investigations

Behrens et al. (2010) describe measurements from a sodar compared with a mast along a ridge in very complex terrain. The sodar had one vertical beam, and four beams each tilted 17.5 ° from the vertical in vertical planes spaced 90 ° in azimuth. Winds were derived from two adjacent tilted beams and the vertical beam, giving four possible winds derived from three beams. This mode of operation was carefully calibrated first over homogeneous terrain. In the complex situation, statistically significant differences were found in these winds over the radius D. An attempt was made to model this with

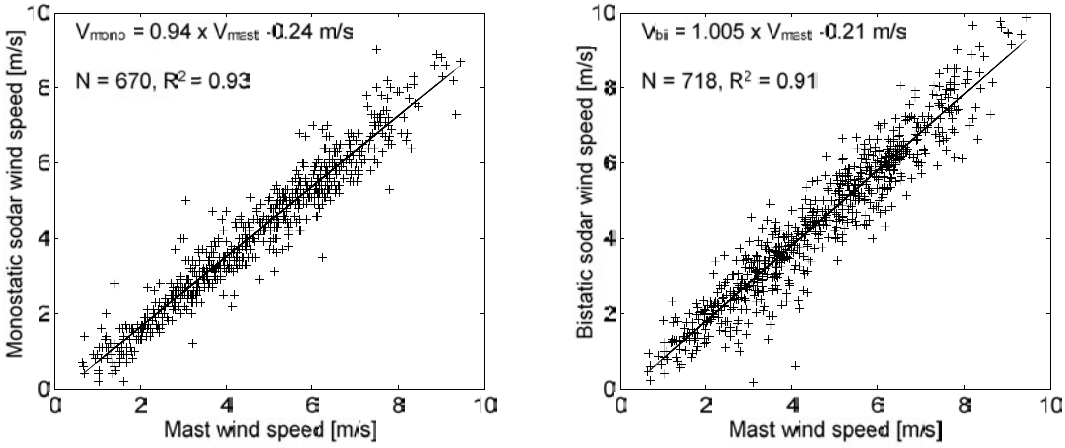

Figure 7: An example of bistatic sodar operation in complex terrain. The comparison is with mast instrumentation at 80 m above a complex ridge. The number of data points in each plot is the N value shown. The monostatic sodar (left plot) underestimates the wind speed, in comparison with the mast, by 6 %, whereas the bistatic sodar (right plot) is within 0.5 % of the mast wind (Strehz and Bradley 2014).

WAsP, but the uncertainties in WAsP were greater than the observed wind spatial variations of about 0.14 m/s. Spatial coherence of the wind speed was also examined by correlating wind components recorded on an upwind beam with the component recorded on a downwind beam. The spatial coherence fell off faster with distance in the homogeneous terrain situation.

As discussed in Section 5 above, Behrens et al. (2012) also modelled their sodar measurements with the simple potential flow model of Section 3, and with two CFD models. The measured underestimation of wind by the sodar on a ridge agreed closely with model predictions, as shown in Fig. 5 above.

Lidar measurements in complex terrain, and their corrections, are discussed by a number of authors (Bezault et al., 2012; Bingöl et al., 2009b,a; Foussekis et al., 2009; Harris et al., 2010; Jeannotte et al., 2014; Friman, 2011; Palma et al., 2008; Rovers, 2012). Foussekis et al. (2009) conducted measurements at the same site with three lidars. They found all lidars underestimated by about 6 %. The lidar beam angle α was found to have little influence on this underestimation, as expected from the discussion in Section 2, but a smaller α resulted in larger variance in measured horizontal wind speed. Harris et al. (2010) and Friman (2011) found CFD corrections were very good, and WsAP less so if the wind flow was over more complex terrain. In common with other studies, while the underestimation can be corrected, the coefficient of determination (a measure of goodness of fit) between lidar and mast data was unchanged by CFD corrections. This means the non-systematic variations do not appear to arise from the topographical spatial variations. For measurements conducted on a complex plateau, Jeannotte et al. (2014) found the underestimation to be less than 1.5 % and corrections with OpenFOAM were not advantageous. A very comprehensive study of underestimation by a continuous-transmission (or CW) lidar in eight measurement campaigns has been provided by Pitter et al. (2012). Underestimation by 1 % to 11 % was corrected to better than 2 % using a CFD model. Corrections for lidar and sodar were found to be similar by Rovers (2012), CFD correcting an underestimation of −5 % to +2 %, and an underestimation of −3 % to +1 % (note that over-correction occurs in some cases).

Bradley et al. (2012b) and Lang and McKeogh (2011) both describe sodar and lidar measurements at the moderately complex Myres Hill experiment. Some results are shown in Fig. 8. Corrections were made using the potential flow model of Section 3. It can be seen that these remote sensing methods could be corrected at this site so as to end up agreeing with the mast winds to within about 1.5 %.

7 Conclusions

For complex terrain sites there are still challenges in using models alone to predict winds sufficiently well for wind energy. This means that, for the foreseeable future, measurements will need to be made at potential or existing sites. Given the hub height and, more significantly, the swept area of present and future turbines, direct measurements from mast mounted instrumentation is now no longer practical. This means that remote sensing techniques are required. Currently these methods are use of sodars or lidars. Commercially available versions of these instruments all use sampling from a number of discrete spatially separated volumes in order to construct the three vector components of the wind at any given height. This process has long been known to give rise to errors in estimated wind because the wind field in complex terrain is not homogeneous.

The present paper reviews the status of obtaining high quality wind estimates from remote sensing instruments in complex terrain. In most cases this involves

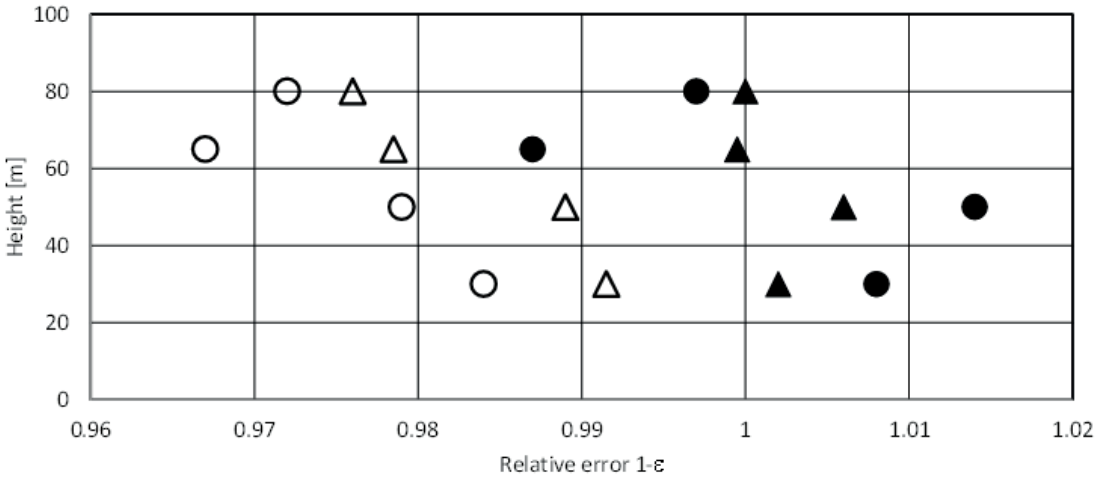

Figure 8: Raw lidar wind speed divided by mast wind speed (open circles) and corrected values (filled circles), and raw sodar wind speed divided by mast wind speed (open triangles) and corrected values (filled triangles) from Bradley et al. (2012b).

using a flow model to estimate the variations in wind components which will be measured by the remote sensing instrument. It is clear from our review that only *relative* variations are required from the model, since the remote sensing instrument obtains a relative wind speed entirely adequately. The result is that generally the corrections required are quite small (typically a few per cent), and there is some evidence in the literature that linear models can make such corrections to the extent required. In cases where there is recirculating detached flow, linear models will give spurious results and CFD, or possibly LES models, are required. The question arises though, as to whether such conditions are ever suitable for turbines.

Some insight into the factors governing lidar and sodar errors can be gained by simple geometric considerations, as discussed in Section 2. In particular, it is clear that the principal governing variable is the curvature of the streamline through the sampling volumes. A first, very rough, guess of this radius of curvature can be obtained from the curvature of the local terrain. However, it is readily shown even with the simplest linear potential flow model (Section 3) that the blocking by a hill, and accompanying speed up over the crest of a hill generally makes the streamline curvature substantially larger than the hill curvature. In other words a flow model is definitely needed.

There have been a number of measurement campaigns in which wind data is obtained at various heights by both masts and remote sensing instruments in complex terrain, followed by applying corrections from models to gauge the accuracy possible from remote sensing measurements. Generally the finding is that linear models do not perform as well as more complicated models, although there are occasions in which the linear models perform better, possibly because of errors in the terrain surface parameters input to the more complicated models. Also, in some instances the models have over-corrected. However, it would seem that remote sensing by either sodar or lidar, corrected with a flow model, can give wind estimates to better than about 1.5 %.

Some caveats should be applied to the above assessment. In particular, very little attention appears to have been given in the literature to atmospheric stability, and the possibility of features such as low level jets (Emeis 2014a,b). Potential flow models effectively assume neutral atmospheric stability, but a number of CFD model investigations have also been restricted to this regime. Also, in reviewing the measurement campaigns it is evident that some model corrections are more successful than others, for comparable terrain complexity. This may be that the terrain complexity has not been sufficiently specified but, before remote sensing instruments can be used completely without support from some mast measurements, it would be good to have clarity on this. Furthermore, mast heights in complex terrain are virtually in all cases limited to 80 m, so the effectiveness of model corrections is not being tested above that height. Intuitively it might be expected that corrections would be smaller at greater heights, but this is not necessarily the case if there are wave phenomena.

Given the necessity to correct estimates from current commercially available remote sensing instruments, it is not surprising that other instrument configurations are being considered. These include bistatic sodars and multi-lidar systems, both of which obtain the wind vector components from within one volume at each height. These systems are still under development, and it is too early to be certain whether they will be cost effective and operationally viable.

References

Afek, I., N. Sela, N. Narkiss, G. Shamai, S. Tsadka, 2013: Wind measurement via direct detection lidar. – SPIE Remote Sensing, 889404–889404.

Ayotte, K.W., 2008: Computational modelling for wind energy assessment. – J. Wind Enginer. Indust. Aerodyn. **96**, 1571–1590.

Bechmann, A., N.N. Sørensen, 2010: Hybrid RANS/LES method for wind flow over complex terrain. – Wind Energy, **13**, 36–50.

Bechmann, A., J. Berg, J. Mann, P.-E. Réthoré, 2011: The Bolund experiment, particular II: blind comparison of microscale flow models. – Bound.-Layer Meteor. **141**, 245–271.

Behrens, P., S. Bradley, T. Wiens, 2010: A multisodar approach to wind profiling. – J. Atmos. Oceanic Technol. **27**, 1165–1174.

Behrens, P., J. O'Sullivan, R. Archer, S. Bradley, 2012: Underestimation of monostatic sodar measurements in complex terrain. – Bound.-Layer Meteor. **143**, 97–106.

Berg, J., J. Mann, A. Bechmann, M. Courtney, H.E. Jørgensen, 2011: The Bolund Experiment, Part I: Flow over a steep, three-dimensional hill. – Bound.-Layer Meteor. **141**, 219–243.

Bezault, C., S. Sanquer, M. Nadah, 2012: Correction tool for Lidar in complex terrain based on CFD outputs. – Proceedings, EWEA.

Bingöl, F., J. Mann, D. Foussekis, 2009a: Conically scanning lidar error in complex terrain. – Meteorol. Z. **18**, 189–195.

Bingöl, F., J. Mann, D. Foussekis,2009b: Lidar performance in complex terrain modelled by WAsP. – Engineering. Proceedings of the European Wind Energy Conference.

Bradley, S., 2007: Atmospheric Acoustic Remote Sensing: Principles and Applications. – CRC Press.

Bradley, S., 2012: A simple model for correcting sodar and lidar errors in complex terrain. – J. Atmos. Ocean. Technol. **29**, 1717–1722.

Bradley, S., S. von Hünerbein, T. Mikkelsen, 2012a: A Bistatic Sodar for Precision Wind Profiling in Complex Terrain. – J. Atmos. Ocean. Technol. **29**, 1052–1061.

Bradley, S., Y. Perrott, P. Behrens, A. Oldroyd, 2012b: Corrections for wind-speed errors from sodar and lidar in complex terrain. – Bound.-Layer Meteor. **143**, 37–48.

Butler, J., F. Quail, 2012: Comparison of a 2nd generation lidar wind measurement technique with CFD numerical modelling in complex terrain. – 2nd International Conference on SuperGen, Hangzhou, China, September 2012, 4. MATLAB

Diebold, M., C. Higgins, J. Fang, A. Bechmann, M.B. Parlange, 2013: Flow over hills: a large-eddy simulation of the bolund case. – Bound.-Layer Meteor. **148**, 177–194.

Eggert, M., 2013: Accurate wind velocity measurements. Traceable doppler lidar system for wind potential analysis and power curve characterisation of wind turbines. – http://www.ptb.de/cms/fileadmin/internet/publikationen/ptb_news/pdf/englisch/news_1_2013_en.pdf

Emeis, S., 2014a: Current issues in wind energy meteorology. – Meteor. Appl. **21**, 803–819.

Emeis, S., 2014b: Wind speed and shear associated with low-level jets over Northern Germany. – Meteorol. Z. **23**, 295–304.

Emeis, S., M. Harris, R.M. Banta, 2007: Boundary-layer anemometry by optical remote sensing for wind energy applications. – Meteorol. Z. **16**, 337–347.

Feng, J., W.Z. Shen, 2014: Wind farm layout optimization in complex terrain: A preliminary study on a Gaussian hill. – J. Physics: Conference Series 524, 012146.

Foussekis, D., T. Georgakopoulos, I. Karga, 2009: Investigating wind flow properties in complex terrain using 3 lidars and a meteorological mast. – EWEC Proceedings.

Friman, M., 2011: Directivity of sound from wind turbines. – Thesis for the degree of Master of Science, The Marcus Wallenberg Laboratory,

Harris, M., I. Locker, N. Power, N. Douglas, R. Girault, C. Abiven, O. Brady, 2010: Validated adjustment of remote sensing bias in complex terrain using CFD. – European Wind Energy Conference.

Jackson, D., J. Beyers, K. Lynch, J. Cooper, A. Baas, I. Delgado-Fernandez, 2011: Investigation of three-dimensional wind flow behaviour over coastal dune morphology under offshore winds using computational fluid dynamics (CFD) and ultrasonic anemometry. – Earth Surface Processes and Landforms **36**, 1113–1124.

Jackson, P., J. Hunt, 1975: Turbulent wind flow over a low hill. – Quart. J. Roy.Meteor. Soc. **101**, 929–955.

Jafari, S., N. Chokani, R. Abhari, 2012: An immersed boundary method for simulation of wind flow over complex terrain. – J. Solar Energy Enginer. **134**, 011006.

Jeannotte, E., C. Masson, D. Faghani, M. Boquet, B. Boucher, E. Osler, 2014: Estimation of LiDAR error over complex terrain covered with forest using numerical tools. – Mechanics & Industry **15**, 169–174.

Lang, S., E. McKeogh, 2011: LIDAR and SODAR measurements of wind speed and direction in upland terrain for wind energy purposes. – Remote Sens. **3**, 1871–1901.

Mann, J., S. Ott, B.H. Jørgensen, H.P. Frank, 2002: WAsP engineering 2000. – Technical Report R–1356(EN), Risø National Laboratoty.

Mikkelsen, T., S. Bradley, 2011: Lidar remote sensing. Int. – Sustainable Energy Rev. **5**, 2–7

Mikkelsen, H. Ejsing Jørgensen, L. Kristensen, 2007: The Bistatic Sodar "Heimdall", You blow, I listen. – Risø National Laboratory.

Mortensen, N.G., A.J. Bowen, I. Antoniou, 2006: Improving WAsP predictions in (too) complex terrain. – EWEC Proceedings.

Palma, J., F. Castro, L. Ribeiro, A. Rodrigues, A. Pinto, 2008: Linear and nonlinear models in wind resource assessment and wind turbine micro-siting in complex terrain. – J. Wind Enginer. Indust. Aerodyn. **96**, 2308–2326.

Pitter, M., C. Abiven, K. Vogstad, M. Harris, W. Barker, O. Brady, 2012: Lidar and computational fluid dynamics for resource assessment in complex terrain. – Proceedings, EWEA.

Prospathopoulos, J., E. Politis, P. Chaviaropoulos, 2012: Application of a 3D RANS solver on the complex hill of Bolund and assessment of the wind flow predictions. – J. Wind Enginer. Indust. Aerodyn. **107**, 149–159.

Rasouli, A., H. Hangan, 2013: Microscale Computational Fluid Dynamics Simulation for Wind Mapping Over Complex Topographic Terrains. – J. Solar Energy Enginer. **135**, 041005.

Rovers, T., 2012: Correction of sodar wind speed bias in complex terrain situations. – Proceedings, EWEA.

Strehz, A., S. Bradley, 2014: Mast comparisons for a new bistatic SODAR design. – http://isars2014.org/wp-content/uploads/2013/11/NTECH2.pdf

Vuorinen, V., A. Chaudhari, J.-P. Keskinen, 2015: Large-eddy simulation in a complex hill terrain enabled by a compact fractional step OpenFOAMsolver. – Adv. Engineer. Software **79**, 70–80.

Wakes, S.J., T. Maegli, K.J. Dickinson, M.J. Hilton, 2010: Numerical modelling of wind flow over a complex topography. – Environ. Modelling & Software **25**, 237–247.

Xu, C., C. Li, J. Yang, W.Z. Shen, Y. Zheng, D. Liu, 2013: Prediction of wind energy distribution in complex terrain using CFD. – International Conference on aerodynamics of Offshore Wind Energy Systems and wakes (ICOWES 2013), 549–557.